PH DEPENDENT STRUCTURAL, OPTICAL AND ELECTRICAL PROPERTIES OF PBS NANOCRYSTALLINE FILMS

Bhaskar Jyoti Baruah[1*],

Keywords:

PbS;
pH;
Nanocrystalline Films;
Chemical bath deposition;
Urbach Energy.

Abstract

Nanocrystalline films of PbS has been deposited on glass substrates by chemical bath deposition method and the effect of pH on the films has been studied. With the increase of pH, the crystallite size increased with the reduction of microstrain and Urbach energy, the direct band gap decreased, and conductivity improved with the maximum value being 5.08×10^{-3} $(\Omega cm)^{-1}$. The films deposited at pH=12.46 become highly absorbing in the wavelength range of 350-800 nm. This film has also shown highest reflectance which was uniforrm in between 320 to 660 nm.

Author correspondence:

First and Corresponding Author

[1] Department of Physics, D. R. College, Goaghat, Assam- 785621, India;

1. Introduction

PbS is a narrow band gap semiconductor having the value of bandgap 0.37–0.4 eV [1] in the bulk state at 300 K. Its relatively large excitonic Bohr radius of 18–20 nm [2] makes it ideal material for band gap tuning and relevant in optoelectronics [3–7].

For synthesis of nanocrystalline thin films, chemical bath deposition (CBD) method is widely used due to its simplicity, cost effectiveness and suitability for large area deposition on substrates [8–17]. The properties of the films deposited by chemical bath deposition method are very sensitive to deposition parameters such as pH. A number of researchers already published their works regarding the effect of pH on the properties of chemically deposited PbS nanocrystalline films [18-24]. But differences in results are noticed. For example, Preetha et.al [20] recorded maximum conductivity at that value of pH which produced maximum microstrain. On the other hand, Remadevi et.al [21] observed the electrical conductivity to be maximum at the pH which produced minimum microstrain. Therefore, we intended to study how pH affects the structural, optical and electrical properties of the PbS nanocrystalline films prepared under our own chosen experimental parameters.

[1] Department of Physics, D. R. College, Goaghat, Assam- 785621, India

2. Experimental Details

2.1 Preparation of the films

Four numbers of different baths were taken. 5 ml solution of 0.5M $Pb(CH_3COO)_2.3H_2O$ were poured into these baths. Then 2ml of 1M triethanolamine (TEA) was added to each of these solutions of $Pb(CH_3COO)_2.3H_2O$ and stirred for 10 minutes. Then NaOH solutions of concentration 2M were added to all the baths dropwise by different amount to set the pH of these baths at 8.22, 9.11, 10.70 and 12.46 respectively. Then after inserting the chemically and ultrasonically cleaned glass substrates, 6 ml of 1M thiourea were added to all these four baths and the baths were topped up with distilled water in order to make the total volume of 100 ml. After two hours of deposition at room temperature (30^oC), the films were taken out of the baths, washed with doubly distilled water, dried and stored in vacuum desicator filled with silica gel. The sides of the substrates facing the walls of the beaker were retained for characterization and the other sides were removed with the help of a dilute acid. The films were coded as pH 8.22, pH 9.11, pH 10.7 and pH 12.46 respectively depending upon the magnitudes of pH at which the deposition took place.

2.2 Characterization of the films

The pH was measured by Eutech pH700 digital meter. The X ray diffraction pattern of the films were recorded by Rigaku Ultima IV X-ray diffractometer at room temperature with CuKα radiation having wavelength 1.5406Å. The surface morphology and energy dispersive X-ray analysis (EDX) were studied by FEI Quanta 250 scanning electron microscope. The optical absorbance, transmittance and reflectance were measured by Hitachi U-3900 UV-Vis spectrophotometer. The current-voltage characteristics were recorded by Keithley 2400 Electrometer using gap type silver electrodes.

3. Results and Discussion

3.1 Structural Properties of the films by XRD

The X-ray diffraction pattern of the films are shown in the fig. 1. Comparison with ICDD card No. 78-1900, the pattern is confirmed as that of polycrystalline film of PbS having fcc structure. It has been observed that the crystallinity got better at higher values of pH as evidenced by the increased intensities of the XRD peaks. The preferred orientations of pH 8.22 – 10.7 films are (111) planes but at pH 12.46, the crystallites prefer to grow along the (200) plane . The intensity of (200) peak is 1.75 times that of (111) peak for pH 12.46 film while at other values of pH, this ratio is less than one. A number of peaks become distinct at pH =12.46 which are not visible at lower values of pH. It is indication of good crystallinity of the film grown at pH=12.46. Calculation of crystallite sizes from the Debye-Scherrer formula shows that the crystallites become bigger as pH increases. The values of crystallite sizes are 31.65, 35.60, 38.67 and 42.37 nm as pH equals 8.22, 9.11, 10.70 and 12.46 respectively. The microstrain (ε) and dislocation density (ρ) are calculated from [25, 26]

$$\varepsilon = \frac{\beta cot\theta}{4} \tag{1}$$

$$\rho = \frac{15\varepsilon}{aD} \tag{2}$$

where β is the fwhm of the XRD peak at the angle of diffraction 2θ, a and D are the lattice constant and the crystallite size respectively. It is observed that both the microstrain and the dislocation density decreases with the increase of pH [Table 1]. This once again confirms that a film of good crystallinity can be obtained at higher values of pH.

NaOH plays two different roles. Triethanolamine complexes the Pb^{2+} ions. NaOH adds stability to this complex by forming lead hydroxocomplex ions. In this way, it slows down the reaction rate by arresting available lead ions. On the other hand, the OH^- ions desulfurate thiourea and produce free S^{2-}s in the solution and thereby accelerate reaction rate. Thus, a good quality PbS film will be formed at that value of pH at which there is balance between the complexation of Pb^{2+}s and generation of S^{2-}s. Now, from analysing the structural properties emerging out of the XRD patterns of the films, it can be understood that at lower values of pH (e.g pH=8.22), the nucleation rate exceeds the growth rate. This results in films having smaller crystallites and larger microstrains. But as pH increases and it reaches a value of 12.46, the Pb^{2+}s are released very slowly and the reaction proceeds at a much controlled rate. Then the density of nucleation is smaller but the growth rate is adequate. Hence, the resulting film is thicker with bigger crystallites and

reduced strain. The thickness of the films, as determined by the gravimetric method, are 510, 525, 905 and 1000 nm for pH 8.22, pH 9.11, pH 10.7 and pH 12.46 respectively.
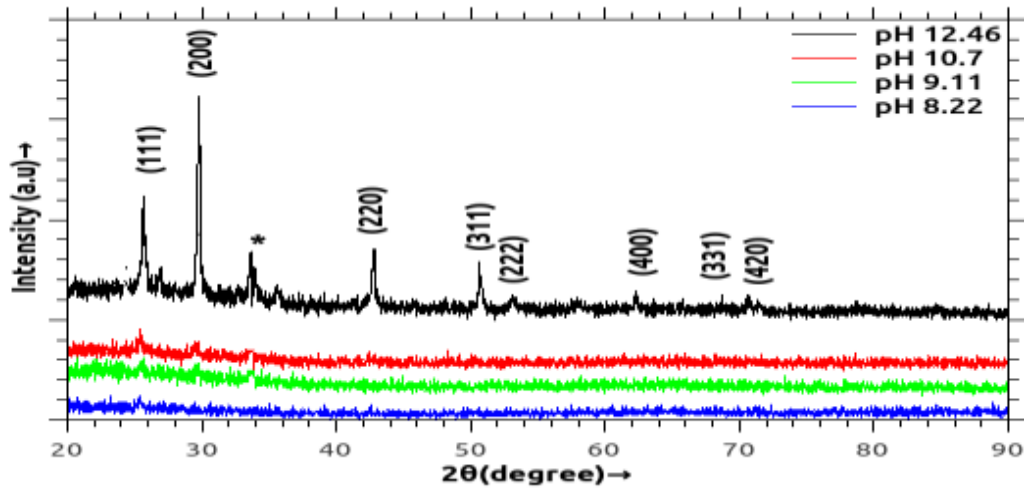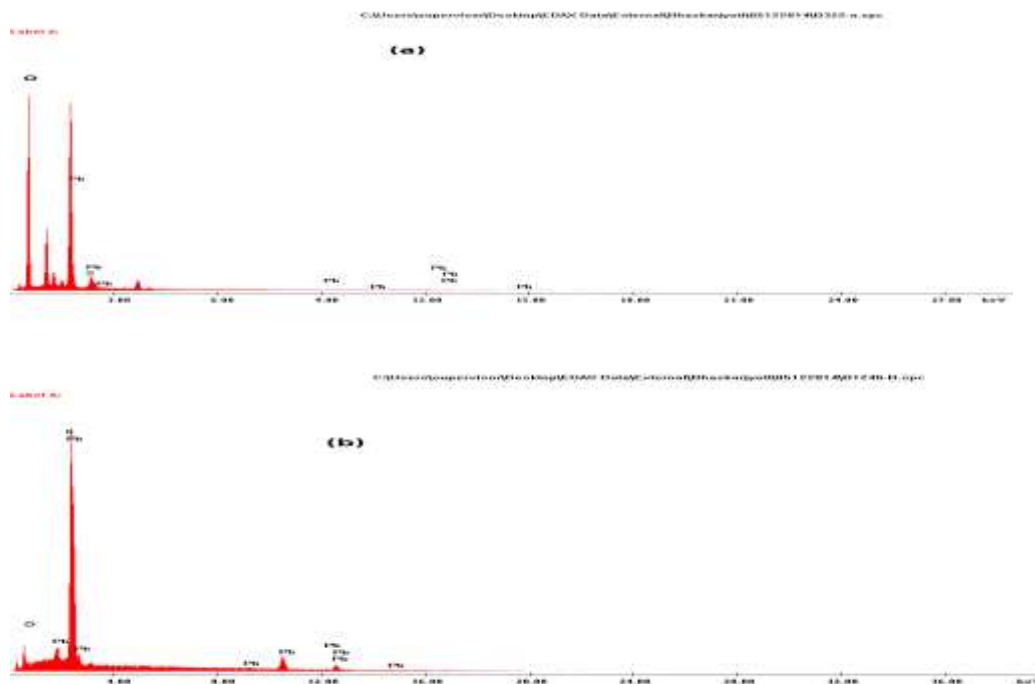

Fig.1: XRD pattern of the films deposited at various pH

Fig.2: EDX spectra of the films deposited at pH (a) 8.22 and (b) 12.46

In the fig. 1, the XRD peak marked * represents some impurity phase resulting from oxidation of PbS or lack of perfect stoichiometry of the films. The Pb:S elemental ratio, as measured by the EDX spectra comes out 0.50 for pH 8.22 and 1.25 for pH 12.46 films [Fig. 2(a) and (b)]. The films are far away from perfect stoichiometry. At pH =8.22, the film is S rich while at pH= 12.46, it is Pb rich. The oxygen content of the pH 8.22 film is much larger than that of the pH 12.46 film. It may be due to higher dangling bond density in the pH 8.22 film.

3.2 Surface Morphology

The surface morphology of the films pH 8.22 and pH 12.46 are shown in Fig 3(a) and (b). The grains of pH 8.22 are nearly spherical while those of pH 12.46 are elongated. That is the grains change their shape at different values of pH. The surface of the pH 12.46 film is uniform and dense with grains but in case of the pH 8.22 film, the substrate is not uniformly coverd with grains. In contrast to the compactness of the pH 12.46 film, the grains of the pH 8.22 film are separated from each other. Agglomeration of crystallites to form larger grains at the surface have been observed in the SEM photographs.
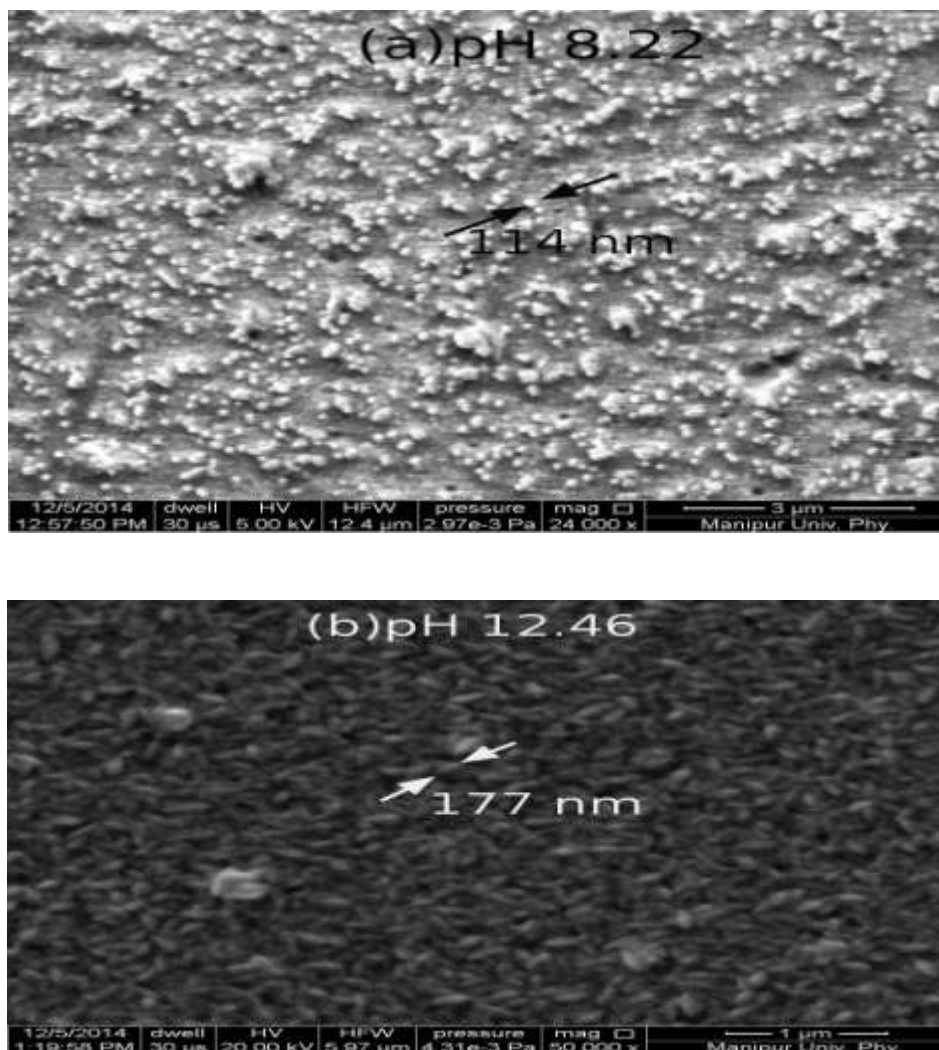

Fig.3: SEM image of the films deposited at pH (a) 8.22 and (b) 12.46

3.3 Optical Properties of the Films by UV-Visible Spectrophotometer:

The absorbance (A), transmittance (T) and the reflectance (R) of the films in the 350-800 nm wavelength range are shown in Fig. 4 (a)-(c). The pH 12.46 film shows highest absorbance and reflectance with least transmittance.Highest absorbance of the pH 12.46 film is due to its highest thickness and crystallite size. From the absorbance spectra [Fig. 4 (a)], it is noticed that the pH of the films play very important role in determining the absorption properties. As pH increases, the absorbance also increases. The exception is pH 8.22 and pH 9.11 where the absorbance of pH 8.22 is larger than pH 9.11.

The pH 9.11 film shows highest transmittance (55%-73%) and the pH 12.46 film shows the least (0-5%) [Fig. 4(b)]. All the films have tedency to become more transparent at higher wavelength. The pH 8.22

and the pH 9.11 films have nearly the same slope of increase in transmittance with wavelength but for the pH 10.7 film, this increase is steeper. The transmission of light through the films are determined by the thickness and crystallite sizes. Greater the thickness and larger the crystallites, smaller is the transmittance.

The reflectance of pH 12.46 film is uniform at 30% from 320 to 660 nm and then it increases slightly with wavelength [fig.4(c)]. The region of uniform reflectance of the other films are narrower and beyond this region, all the films show increase in reflectance with wavelength. The slope of this increase is maximum in pH 10.7 film. It's reflectance increased from 3% at 460 nm to 33% at 800 nm. The film which gives maximum reflectance at all wavelengths is the pH 12.46 film. This implies that this film has the surface uniformity better than the other films. The fact that the pH 12.46 film has the uniform coverage on the substrate has also been evident from the SEM image of the films [Fig.3(b)].

The absorption edge of all the films are obtained in the visible region, a marked blue shift from the bulk value (3020 nm), indicating quantum confinement. The direct band gaps of the films are obtained as 2.00, 1.80, 1.68 and 1.62 eV for pH 8.22, pH 9.11, pH 10.7 and pH 12.46 respectively [Fig. 5(a)-(c)]. The decrease of direct band gaps with the increase of pH was also reported in [102, 104-106]. That is, the direct band gaps bear an inverse relationship with the crystallite size – a fact arising due to confinement of electrons and holes in smaller volume.

The values of Urbach energy (E_u), signifying transitions to mid gap states, are calculated from [27]

$$E_u = \frac{1240}{Slope\,of\,the\,linear\,regression\,of\,ln\,A\,vs\quad .1/\lambda}\,(eV) \qquad (3)$$

where A is the absorbance and λ is the wavelength of radiation. These values are calculated as 1.40, 1.24, 0.70 and 0.64 eV respectively for the films pH 8.22, pH 9.11, pH 10.7 and pH 12.46 (fig. 6). The reduction of Urbach energy with the increase of pH implies that the defects in the film decrease at higher values of pH of the deposition bath.

3.4 Current Voltage Characteristics

The Current-Voltage characteristics of the pH 8.22 and the pH 10.70 films over the voltage range -5 to +5 volt and of the pH 12.46 over -0.5 to +0.5 volt have been shown in the fig.7 (a) and (b) respectively. The current-voltage variation behaviour of all the films are linear. The slope of linear regression of this variation gives the conductance of the films which is about 1000 times larger for the pH 12.46 film than the pH 8.22 and pH 10.70 film. The conductivities (σ) of the films are calculated from the formula [28]

$$\sigma = \frac{L}{Rbt} \qquad (4)$$

where R is the resistance of the films as determined from the slope of the current-voltage characteristics, L is the spacing between the electrodes, b is the breadth of the film in between the contacts and t is the thickness of the films. The values of conductivities were obtained as 8.26×10^{-6}, 1.60×10^{-5} and 5.08×10^{-3} (Ω cm)$^{-1}$ respectively for the films pH 8.22, pH 10.70 and pH 12.46. From these data, the pH 12.46 film has been observed to possess relatively good conducting property. It's superiority as a conductor over the other films is the result of good crystallinity, suitable band gap and interconnected grains. The improvement of conductivity with the increase of pH are also reported in [21,23].
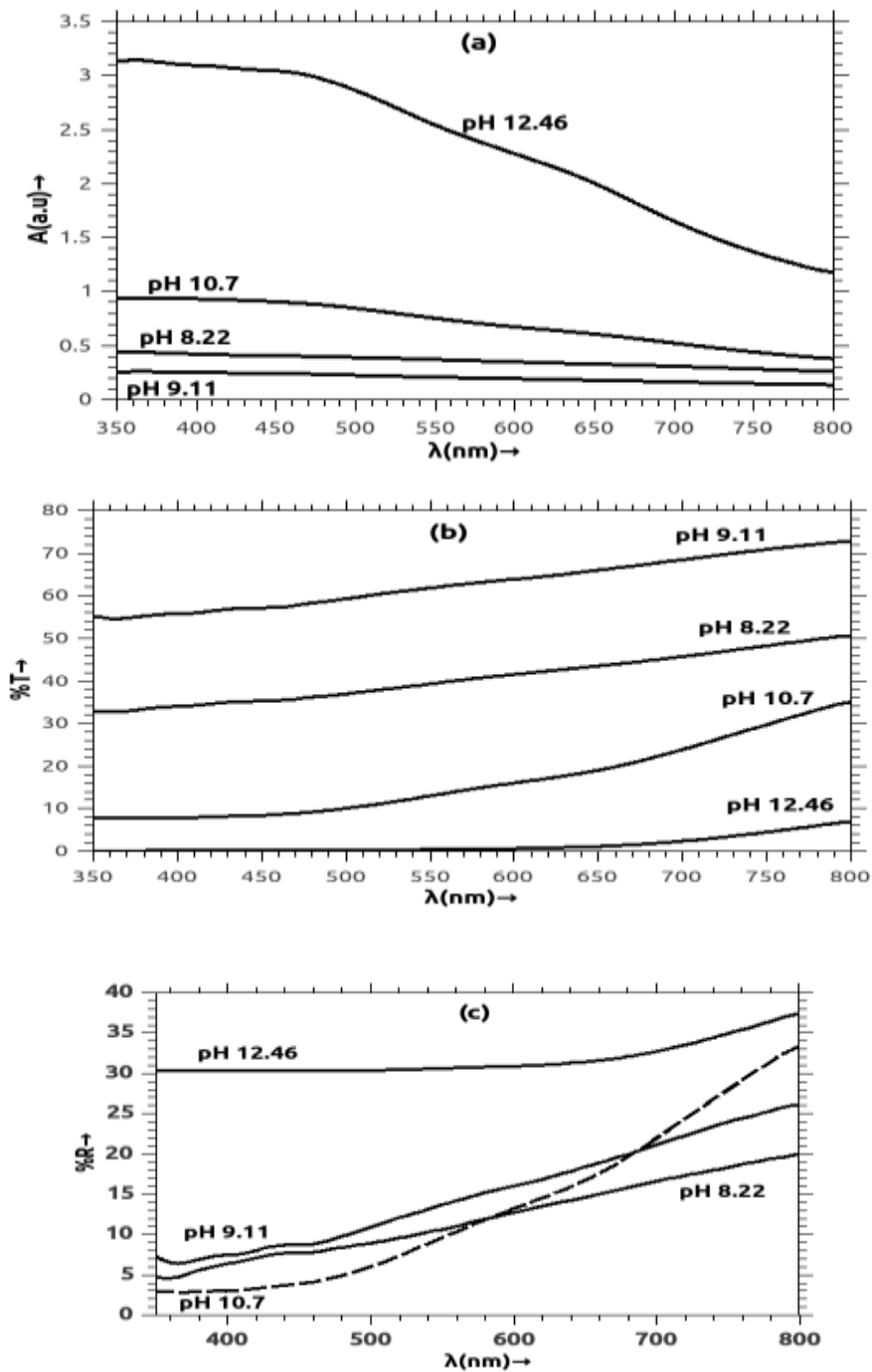
Fig.4: (a) Absorbance, (b) transmittance and (c) reflectance spectra of the films deposited at various pH
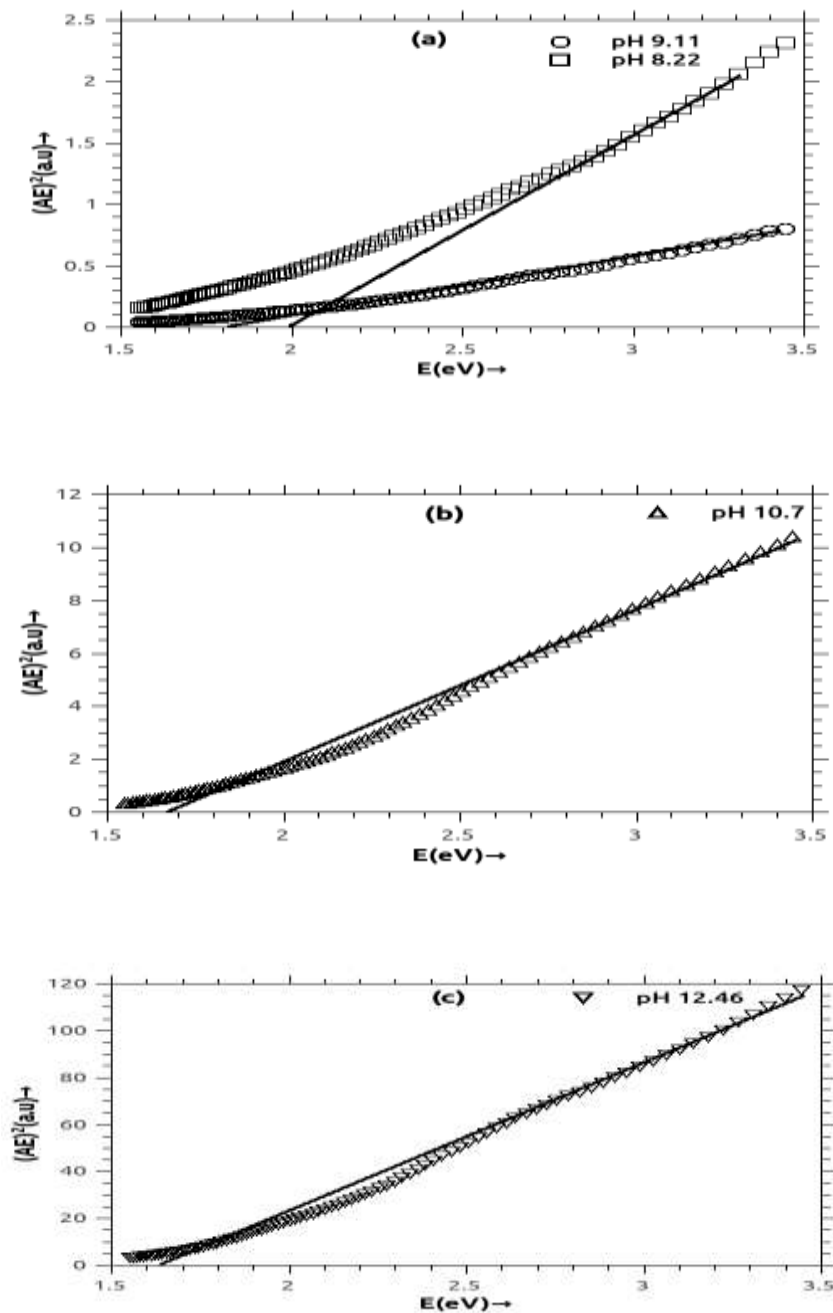
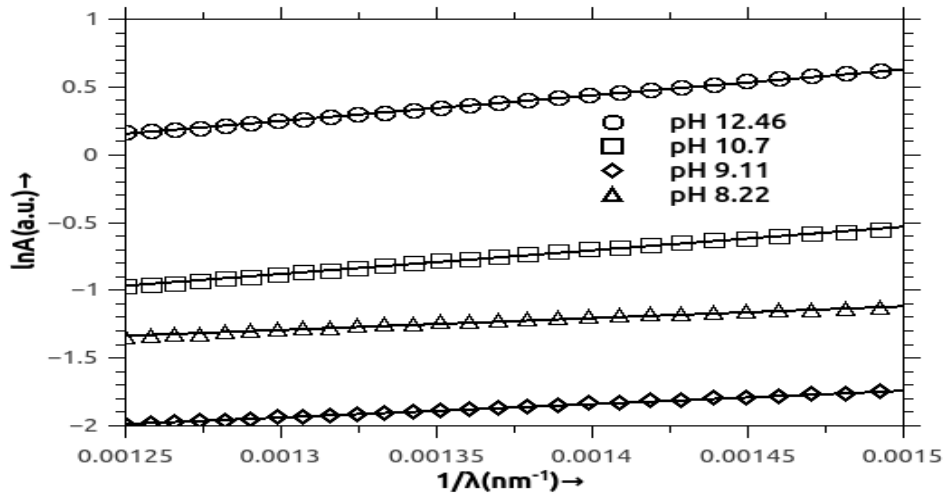Fig 5: Plots to determine direct band gaps of the films deposited at pH (a) 8.22, 9.11, (b)10.7 and (c) 12.46

Fig.6 : lnA vs. 1/λ plot to determine Urbach energies of the films deposited at various pH
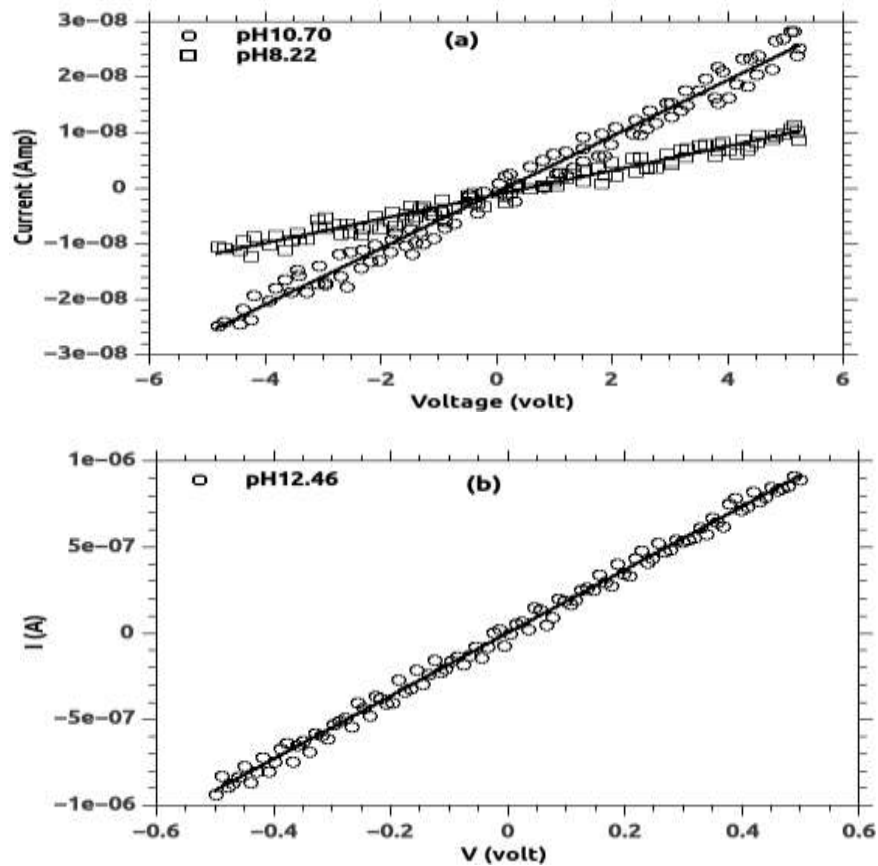

Fig. 7: Current-voltage characteristics of the films deposited at the values of pH (a) 8.22, 10.7, (b) 12.46

Table 1: **Structural, Optical and Electrical Properties of PbS thin film deposited at various pH**

pH	$\varepsilon (\times 10^{-3})$ #	$\rho~(\times 10^{11})$ (cm^{-2}) #	Pb:S (Elemental Ratio)	D (nm) #	E_g (Direct) (eV) #	E_u (eV) #	σ $(\Omega cm)^{-1}$ #
8.22	4.79	4.13	0.50	31.65	2.00	1.40	8.26×10^{-6}
9.11	4.26	3.26	----------	35.60	1.80	1.24	-----------
10.7	4.21	2.75	----------	38.67	1.68	0.70	1.60×10^{-5}
12.46	3.58	2.34	1.25	42.37	1.62	0.64	5.08×10^{-3}

ε = strain; ρ= dislocation density; D=Crystallite Size; E_g(Direct) = Direct Band Gap; E_u=Urbach Energy; σ = Conductivity

4. Conclusions

PbS nanocrystalline films have been prepared with 0.5M lead acetate complexed by 1M TEA and 1M thiourea at 30°C and at four different pH (8.22, 9.11, 10.7, 12.46). The film thickness and crystallite size increased with the increase of pH. The direct band gap reduced from 2.00 eV to 1.62 eV with the increase of pH from 8.22 to 12.46. The optical absorbance became maximum at pH=12.46. Microstrain and Urbach energy decreased with the increase of pH. Electrical conductivity was observed to increase with the increase of pH. The best conductivity of 5.08×10^{-3} $(\Omega cm)^{-1}$ was obtained for pH=12.46.

Acknowledgement

References

1. E. Güneri, F. Göde, S. Çevik, Thin Solid Films 589, 578 (2015)

2. Baligh Touati, Abdelaziz Gassoumi, Salem Alfaify, Kamoun-Turki Najoua, Mater. Sci. Semicond. Process. 34, 82 (2015)

3. N. Choudhury, B.K. Sarma, Thin Solid Films 519, 2132 (2011)
4. P. Yang, C.F. Song, M.K. Lu, X. Yin, G.J. Zhou, D. Xu, D.R.Yuan, Chem. Phys. Lett. 345, 429 (2001)
5. H. Hirata, K. Higoshiyama, Bull. Chem. Soc. Jpn 44, 2420(1971)
6. P.K. Nair, M.T.S. Nair, J. Phys. D 23, 150 (1990)
7. A. Martucci, J. Fick, J. Schell, G. Battaglin, M. Guglielmi, J.Appl. Phys. 86, 79 (1999)
8. A. Hussain, A. Begum, A. Rahman, Indian J. Phys. 86, 697(2012)
9. B. Barman, K.C. Sarma, Indian J. Phys. 86, 703 (2012)
10. R.R. Pawar, R.A. Bhavsar, S.G. Sonawane, Indian J. Phys. 86, 871 (2012)
11. R. Shrivastava, S.C. Shrivastava, R.S. Singh, A.K. Singh, Indian J. Phys. (2015). doi:10.1007/s12648-015-0694-8
12. P.K. Mochahari, K.C. Sarma, Indian J. Phys. 88, 1265 (2014)
13. Y.J. Yang, S. Hu, Thin Solid Films 516, 6048 (2008)
14. S. Kaci, A. Keffous, M. Trari, O. Fellahi, H. Menari, A. Manseri, L. Guerbous, J. Lumin. 130, 1849 (2010)
15. N.B. Kotadiya, A.J. Kothari, D. Tiwari, T.K. Chaudhuri, Appl. Phys. A 108, 819 (2012)
16. M.S. Ghamsari, M.K. Araghi, S.J. Farahani, Mater. Sci. Eng. B 133, 113 (2006)
17. R. Devi, P. Purkayastha, P.K. Kalita, B.K. Sarma, Bull. Mater. Sci. 30, 123 (2007)
18. Chattarki et.al, *Materials Letters* **67** (2012) 39

19. E Yücel, Y Yücel, B Beleli, *Journal of Crystal Growth* **422** (2015) 1
20. K.C. Preetha et.al, *Current Applied Physics* **12** (2012) 53
21. T. L. Remadevi, K. C. Preetha, *J Mater Sci: Mater Electron* **23** (2012) 2017
22. L. Beddek et.al, *International Journal of Scientific Research & Engineering Technology* **3** (2015) 138
23. R K Joshi et.al, *Applied Surface Science* **221** (2004) 43
24. Carrillo-Castillo et.al, *Chalcogenide Letters* **10** (2013) 105
25. Z. Wang, B. A. Bunker, *Phys. Rev. B* **46** (1992), 11277
26. J. C. Mikkelsen, J. B. Boyce, *Phys. Rev. Lett.* **49** (1982) 1412
27. H. Mahfoz Kotb, M.A. Dabban, A.Y. Abdel-latif, M.M. Hafiz, J. Alloys Compd. 512, 115 (2012)
28. A. Goswami, Thin Film Fundamentals (New Age International(P) Ltd., New Delhi, 2008), p. 265